Spatially Localized Self-Injection of Electrons in a Self-Modulated Laser-Wakefield Accelerator by Using a Laser-Induced Transient Density Ramp

T.-Y. Chien,[1,2] C.-L. Chang,[1] C.-H. Lee,[3] J.-Y. Lin,[4] J. Wang,[1,2,5] and S.-Y. Chen[1]

[1]*Institute of Atomic and Molecular Sciences, Academia Sinica, Taipei 106, Taiwan*
[2]*Graduate Institute of Electro-Optical Engineering, National Taiwan University, Taipei 106, Taiwan*
[3]*Research Center for Applied Sciences, Academia Sinica, Taipei 115, Taiwan*
[4]*Department of Physics, National Chung Cheng University, Chia-Yi 621, Taiwan*
[5]*Department of Electrical Engineering, National Taiwan University, Taipei 106, Taiwan*
(Received 16 August 2004; published 24 March 2005)

By using a laser-induced transient density ramp, we demonstrate self-injection of electrons in a self-modulated laser-wakefield accelerator with spatial localization. The number of injected electrons reaches 1.7×10^8. The transient density ramp is produced by a prepulse propagating transversely to drill a density depression channel via ionization and expansion. The same mechanism of injection with comparable efficiency is also demonstrated with a transverse plasma waveguide driven by Coulomb explosion.

DOI: 10.1103/PhysRevLett.94.115003 PACS numbers: 52.38.Kd, 52.35.Mw, 52.38.Mf

Wakefield acceleration of electrons in a plasma has the potential of becoming the next generation particle accelerator [1]. The acceleration gradient of the plasma wave can reach several GeV/cm for $1 \times 10^{19}\ \mathrm{cm}^{-3}$ plasma density [2], which is about 3 orders of magnitude larger than the radio-frequency linac. Such a large gradient holds the promise of a compact high-energy electron source. Electrons can be trapped and accelerated by the plasma wave provided their initial position is at the right phase of the wave and their initial velocity is above a trapping threshold [3]. Self-trapping of electrons has been observed in many experiments in the self-modulated laser-wakefield accelerator (SM-LWFA) regime [4,5], in which a laser pulse with a duration larger than several plasma-wave periods is used to drive the wave through Raman forward scattering (RFS) instability [6]. Plasma-wave breaking [4] and preacceleration of plasma electrons by the slow plasma wave driven by Raman backscattering instability [7] were identified to be the injection mechanisms. Controlled injection by a collinearly propagating prepulse has also been demonstrated [8].

To obtain an electron beam with small-energy spread and short duration, electrons must be injected into a single bucket of the plasma wave at a spatially localized position. This is difficult to achieve with a radio-frequency electron gun. Several optical injection methods have been proposed for precise control of the timing of injection. Umstadter *et al.* proposed that by using the transverse ponderomotive force of a laser pulse crossing the plasma wave perpendicularly, the trajectories of some electrons in the plasma wave can be altered and become trapped [9]. Esarey *et al.* proposed to use the moving beat wave of two colliding pulses with different frequencies to inject electrons into a plasma wave [10]. Kotaki *et al.* proposed to use a counterpropagating pulse of the same frequency to collide with a pump pulse, and electrons are injected by the optical standing wave [11]. By computer simulations all these schemes have been shown to produce a short-duration and small-energy-spread electron beam.

A different category of electron injection schemes involves shaping of the gas target [12–15]. Suk *et al.* proposed that by creating a sharp downward density ramp in the plasma, background electrons can be injected into the plasma wakefield at the ramp. The physical picture is that when a plasma wave is generated across a sharp density down ramp, electrons near the boundary move toward the higher density region and then oscillate back into the lower density region. Since the oscillation period is longer in this region, these electrons are dephased with respect to the background plasma-wave electrons and thus become trapped. For significant self-injection to occur, the scale length of the ramp should be close to or less than the plasma-wave wavelength. In Ref. [15] it was suggested that the wall of a transverse plasma waveguide can serve as the density ramp for self-injection even though its scale length is several times the plasma-wave wavelength. In this Letter, we report the first experimental demonstration of self-injection by a sharp density ramp in a SM-LWFA. By using a transverse prepulse to ionize and heat the gas target locally, a transient density up ramp and a down ramp are created as a result of plasma thermal expansion. The number of injected electrons reaches 1.7×10^8. The same mechanism of injection is also demonstrated with a transverse plasma waveguide driven by an intense prepulse via Coulomb explosion. If a temporally localized plasma wakefield can also be produced by two optimally separated collinear pump pulses as proposed in Ref. [9], the combination is expected to lead to femtosecond single-bucket injection, which is an essential step toward producing high-quality ultrashort-pulse electron acceleration.

A 10 TW, 55 fs, 810 nm, and 10 Hz Ti:sapphire laser system based on chirped-pulse amplification [16] is used in this experiment. After the amplifier chain the pulse is split into two, each going through an energy tuner and a pulse compressor. One serves as the pump pulse for driving a plasma wave, and the other is used as the prepulse for gas jet drilling. The pump pulse is focused by an $f/8$ off-axis parabolic mirror to a focal spot of 8.5 μm diameter in full width at half maximum with 80% energy enclosed in a Gaussian-fit profile. Perpendicular to the pump pulse, the prepulse is focused with an $f/4$ off-axis parabolic mirror to a focal spot of 4 μm diameter with 54% energy enclosed. The 2×10^{19} cm^{-3} helium gas target is produced from a pulsed valve with a supersonic conical nozzle. The density profile has a 1 mm flattop region with 250 μm boundaries. Two side-scattering imaging systems are used to observe the laser channel of the pump pulse by Thomson scattering. The directions of observation are in 90° polar angle and 90° and 18° azimuthal angles, respectively, with respect to the propagation axis of the pump pulse. The 0° azimuthal angle is defined as the direction opposite to the propagation direction of the prepulse. Because the intensity of Thomson scattering is a product of laser intensity and plasma density, the plasma density ramp can be visualized in side-scattering images. Raman forward scattering spectra are measured by collecting the emission with a concave mirror at a 15° angle with respect to the propagation axis of the pump pulse and imaging onto the entrance slit of a spectrometer. The beam profile of the accelerated electrons is measured with a LANEX (Kodak) scintillating screen imaged by a charge-coupled device (CCD) camera [17]. A 25 μm aluminum foil is placed in front of the LANEX screen to block the laser beam. The foil and the back support of the LANEX screen together also block electrons with energy below 100 keV. The electron number is measured by integrating the signals on the LANEX screen, with the absolute number calibrated by using a scintillator-photomultiplier assembly of known sensitivity. The collection angle of electrons is $6.6° \times 13°$. The electron energy spectrum is measured by adding a collimator and a dipole magnet in front of the LANEX screen [17].

For a plasma electron density of 1×10^{19} cm^{-3}, the wavelength of the plasma wave is about 10 μm. A density ramp of this length scale cannot be produced by mechanical shaping of the gas nozzle. In this experiment, we produced such a sharp ramp by using transient laser drilling on the gas jet. A 55 fs, 7 mJ prepulse is used to ionize a transverse plasma column in the gas jet, and 4 ns later after expansion of this plasma column, a density depression channel is formed in the neutral gas. By positioning this channel in the path of the pump pulse, the pump pulse driving a plasma wave is forced to go through sharp ramps for self-injection.

Figure 1(a) shows the images of injected electron beam and side scattering of the pump pulse for various vertical (perpendicular to the plane of the prepulse and the pump pulse) positions of the prepulse focal spot with respect to the pump pulse. The 210 mJ, 260 fs pump pulse is negatively chirped, with its duration optimized for maximum RFS satellite intensity [18]. The image of the injected electron beam is obtained by subtracting the image of the electron beam without the prepulse from that with the prepulse. As shown, a sharp dark zone is present in the laser channel of the pump pulse when the density depression channel intersects it. In addition, bright scattering appears at both the edges of the dark zone, also indicating the presence of sharp density ramps. Such a sharp density ramp is expected since optical field ionization (multiphoton ionization) is a highly nonlinear process with a sharp intensity threshold. As we move the prepulse vertically away from the best overlap position, the dark region becomes smaller as expected from a cylindrical density depression channel. This observation indicates that the

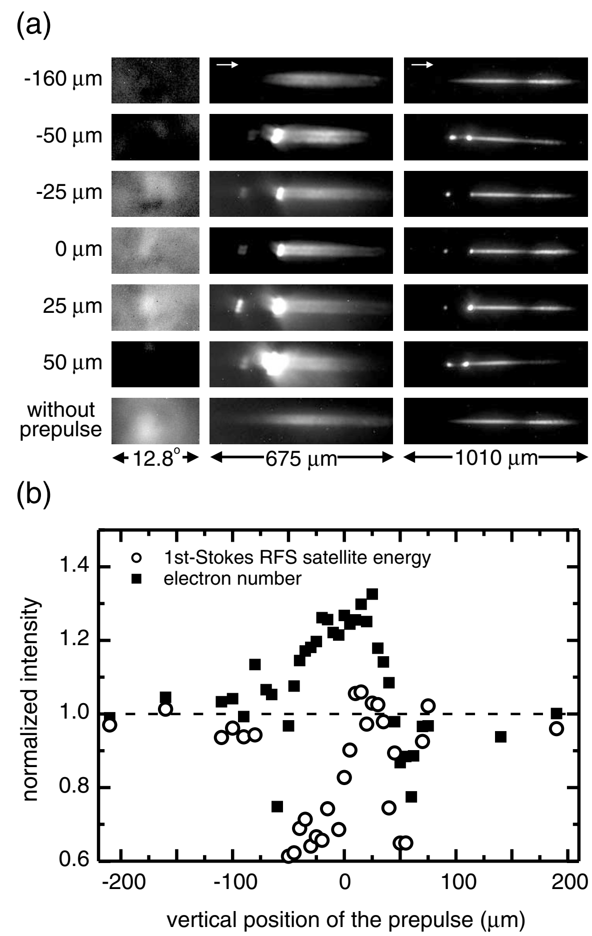

FIG. 1. (a) Images of the electron beam from ramp injection (first column) and 90° (second column) and 18° (third column) side scattering of the pump pulse for various vertical positions of the prepulse with respect to the pump pulse. The prepulse is 7 mJ and 55 fs, the pump pulse is 210 mJ and 260 fs, and the pump pulse delay relative to the prepulse is 4 ns. The helium gas density is 2×10^{19} cm^{-3}. The white arrows indicate the propagation direction of the pump pulse. The electron beam profile and the side-scattering images taken without the prepulse are shown for comparison. (b) First-Stokes RFS satellite energy (open circles) and the number of accelerated electrons (solid squares) as a function of the vertical position of the prepulse. Both signals are obtained by averaging over 100 laser shots on the CCD camera.

vertical spatial extent of the density depression channel is about 140 μm, consistent with the observed width of the dark region. The propagation of the pump pulse is not severely altered when it traverses near the center of the density depression channel, as shown in the side-scattering images for the regions between ± 25 μm. When the prepulse position is displaced by ± 50 μm, the pump pulse deflects, as seen clearly in the 18° side-scattering images, due to the sharp transverse density gradient at the boundaries of the channel. As shown, injection occurs only when sharp density ramps appear in the path of the pump pulse, and the electron beam profile is similar to that from self-trapping.

Figure 1(b) shows the first-Stokes RFS satellite energy and the number of accelerated electrons as a function of the vertical position of the prepulse, both normalized to that without the prepulse. The number of self-trapped electrons without the prepulse is 6.8×10^8. With the prepulse the electron number increases by 25% in the region within ± 25 μm, while the first-Stokes RFS stays the same or is reduced. Both signals drop to about 70% at ± 60 μm, at which the pump beam hits the vertical boundary of the density depression channel. As the prepulse is moved farther away from the pump pulse, both the electron number and the RFS satellite intensity return to the same levels as without the prepulse.

Since the RFS satellite intensity is a measure of the plasma-wave amplitude, the data show the increase of the electron number within ± 25 μm is due to an enhanced electron injection rather than enhanced self-trapping. The vertical spatial extent of the region where the electron number increases correlates well with the observation of the density depression zone in the side-scattering image. This correlation identifies that the additional electrons are injected by the density ramps. To self-trapping the density depression zone causes the opposite effect because in the zone the trapping threshold is much higher. The ramp scale length can be estimated from the distance between the edges of the high-density region and the density depression zone in the lineout of the side-scattering image of the pump pulse. From Fig. 1 the distance from the edge of the high-density region to the position of 75% of its density is 5.5 μm (19.8 μm at 10%), which is very close to the plasma-wave wavelength of the high-density region (5.2 μm). This is consistent with Ref. [14], in which the simulation shows that electron injection occurs for a ramp of length equal to or less than one plasma-wave wavelength with a high-density region of 5×10^{18} cm^{-3} density and a ratio of 75% between the plasma densities of the low-density and the high-density regions. In addition, no dependence of the electron number on the polarization of the two pulses is observed. The relative temporal position of the pulses and the polarization independence rule out all the optical injection mechanisms described in the second paragraph.

Since the density profile encountered by the pump pulse is a combination of the preformed plasma and the residual neutral gas, the density ramp should become sharper with time as the preformed plasma expands outward and dissipates on the nanosecond time scale. Figure 2 shows the first-Stokes RFS satellite energy and the number of accelerated electrons as a function of the pump pulse delay. The inset of Fig. 2 shows the corresponding images of the injected electron beam and side scattering of the pump pulse. As shown, the fraction of ramp-injected electrons increases from 0% at 67 ps to 25% at 4 ns, which verifies the prediction of Ref. [13] that a sharper density ramp

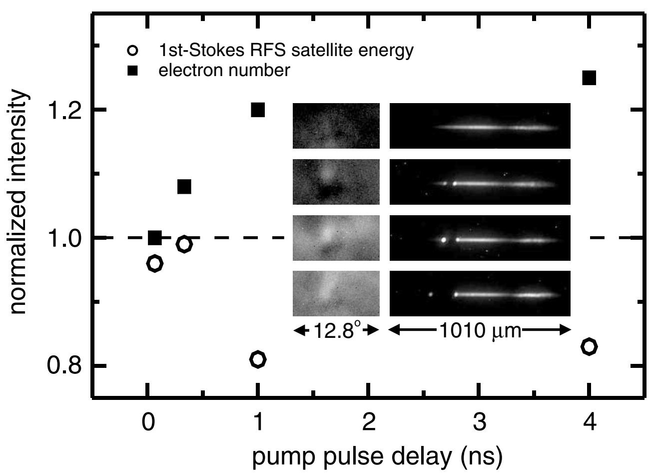

FIG. 2. First-Stokes RFS satellite energy (open circles) and the number of accelerated electrons (solid squares) as a function of pump pulse delay for the zero vertical position of the prepulse. The inset shows the images of the electron beam from ramp injection (first column) and 18° side scattering of the pump pulse (second column) for a pump pulse delay of 67 ps, 333 ps, 1 ns, and 4 ns (from the first to the fourth row). Other parameters are the same as that described in Fig. 1.

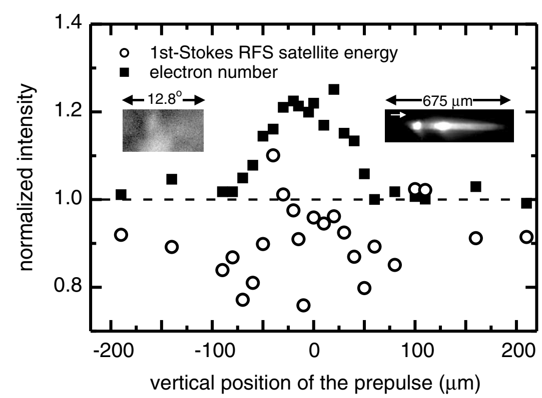

FIG. 3. First-Stokes RFS satellite energy (open circles) and the number of accelerated electrons (solid squares) as a function of the vertical position of the prepulse. The insets show the profile of the ramp-injected electron beam (left) and 90° side scattering of the pump pulse (right) for the zero vertical position of the prepulse. The prepulse is 80 mJ and 55 fs, the pump pulse is 210 mJ and 260 fs, and the pump pulse delay is 67 ps. The helium gas density is 2×10^{19} cm^{-3}.

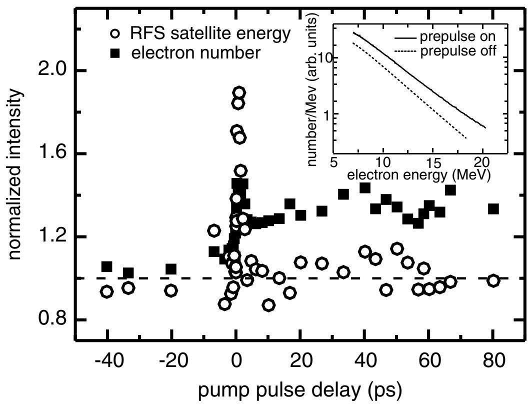

FIG. 4. First-Stokes RFS satellite energy (open circles) and the number of accelerated electrons (solid squares) as a function of the pump pulse delay for the zero vertical position of the prepulse. The inset shows the electron energy spectra with (solid line) and without (dashed line) the prepulse at a pump pulse delay of 67 ps. Other parameters are the same as that described in Fig. 3.

enhances electron injection. In contrast, the RFS satellite energy drops, which can be understood from the shortening of the interaction length for RFS by the density depression channel. In addition, no difference in the propagation of the pump pulse between these cases was shown in the side-scattering images. These observations strongly support our interpretations.

To demonstrate electron injection by a transversely intersecting plasma waveguide as proposed in Ref. [15], the prepulse energy is raised to 80 mJ (peak intensity: 4.1×10^{18} W/cm^2) to drive a plasma waveguide through the Coulomb explosion [19]. The insets of Fig. 3 show the images of the injected electron beam and side scattering of the pump pulse for the zero vertical position of the prepulse. It can be seen clearly that the prepulse has created a plasma density depression channel (plasma waveguide) at a delay of 67 ps. Figure 3 shows the first-Stokes RFS satellite energy and the number of accelerated electrons as a function of the vertical position of the prepulse. As in the case of Fig. 1, the injection of electrons occurs only when the density depression channel intersects the path of the pump pulse, and the number of injected electrons decreases with an increasing displacement of the density depression channel. Again, such a correlation with vertical overlap, the slightly suppressed RFS satellite intensity, and no dependence on laser polarization verify the mechanism of ramp injection by the plasma waveguide. The length scale of the density ramp (< 4 plasma-wave wavelengths) also compares well with the simulation in Ref. [15]. The inset of Fig. 4 shows the electron energy spectra for the cases with and without the prepulse. The continuous distribution instead of a monoenergetic peak for the ramp-injected electrons is expected because, although the electrons are injected in a highly localized region, every bucket in the plasma wave can inject electrons as they traverse the density ramp.

Figure 4 shows the first-Stokes RFS satellite energy and the number of accelerated electrons as a function of the pump pulse delay for the zero vertical position of the prepulse. Ramp injection of electrons with a fraction ranging from 25% to 45% is attained in the region of the pump pulse delay of 0–80 ps. The time scale of the evolution of the plasma density depression channel is consistent with that reported for the plasma waveguide formation driven by the Coulomb explosion [19]. Note that between 0–3 ps the increase of the electron number can reach as high as 70%. However, this increase is clearly due to the enhanced Raman forward scattering instability, since the RFS satellite intensity also increases significantly in this region while no dark zone is observed in the side-scattering image. The underlying physics of such an enhancement of RFS requires further investigation.

[1] T. Tajima and J.M. Dawson, Phys. Rev. Lett. **43**, 267 (1979).
[2] S.P. Le Blanc *et al.*, Phys. Rev. Lett. **77**, 5381 (1996); H. Kotaki *et al.*, Phys. Plasmas **9**, 1392 (2002).
[3] E. Esarey and M. Pilloff, Phys. Plasmas **2**, 1432 (1995).
[4] A. Modena *et al.*, Nature (London) **377**, 606 (1995).
[5] C.A. Coverdale *et al.*, Phys. Rev. Lett. **74**, 4659 (1995); D. Umstadter *et al.*, Science **273**, 472 (1996); A. Ting *et al.*, Phys. Rev. Lett. **77**, 5377 (1996); C. Rousseaux *et al.*, Phys. Plasmas **9**, 4261 (2002); W.P. Leemans *et al.*, Phys. Rev. Lett. **89**, 174802 (2002).
[6] J. Krall, A. Ting, E. Esarey, and P. Sprangle, Phys. Rev. E **48**, 2157 (1993).
[7] P. Bertrand *et al.*, Phys. Rev. E **49**, 5656 (1994); C.I. Moore *et al.*, Phys. Rev. Lett. **79**, 3909 (1997).
[8] W.-T. Chen *et al.*, Phys. Rev. Lett. **92**, 075003 (2004).
[9] D. Umstadter, J.K. Kim, and E. Dodd, Phys. Rev. Lett. **76**, 2073 (1996).
[10] E. Esarey *et al.*, Phys. Rev. Lett. **79**, 2682 (1997).
[11] H. Kotaki *et al.*, Phys. Plasmas **11**, 3296 (2004).
[12] S. Bulanov, N. Naumova, F. Pegoraro, and J. Sakai, Phys. Rev. E **58**, R5257 (1998); R.G. Hemker, N.M. Hafz, and M. Uesaka, Phys. Rev. ST Accel. Beams **5**, 041301 (2002).
[13] H. Suk, N. Barov, J.B. Rosenzweig, and E. Esarey, Phys. Rev. Lett. **86**, 1011 (2001); H. Suk, J. Appl. Phys. **91**, 487 (2002); R.J. England, J.B. Rosenzweig, and N. Barov, Phys. Rev. E **66**, 016501 (2002); M.C. Thompson, J.B. Rosenzweig, and H. Suk, Phys. Rev. ST Accel. Beams **7**, 011301 (2004).
[14] H. Suk, H.J. Lee, and I.S. Ko, J. Opt. Soc. Am. B **21**, 1391 (2004).
[15] J.U. Kim, N. Hafz, and H. Suk, Phys. Rev. E **69**, 026409 (2004).
[16] H.-H. Chu *et al.*, Appl. Phys. B **79**, 193 (2004).
[17] R. Wagner, S.-Y. Chen, A. Maksimchuk, and D. Umstadter, Phys. Rev. Lett. **78**, 3125 (1997).
[18] T.-W. Yau *et al.*, Phys. Plasmas **9**, 391 (2002).
[19] S.-Y. Chen *et al.*, Phys. Rev. Lett. **80**, 2610 (1998).